Biochemical and Biophysical Research Communications 406 (2011) 85–88

Contents lists available at ScienceDirect

Biochemical and Biophysical Research Communications

journal homepage: www.elsevier.com/locate/ybbrc

Head/tail interaction of vinculin influences cell mechanical behavior

Gerold Diez, Vera Auernheimer, Ben Fabry, Wolfgang H. Goldmann *

Center for Medical Physics and Technology, Biophysics Group, Friedrich-Alexander-University Erlangen-Nuremberg, Henkestrasse 91, 91052 Erlangen, Germany

ARTICLE INFO

Article history:
Received 28 January 2011
Available online 3 February 2011

Keywords:
Vinculin
Head–tail interaction
Mutant A50I
Focal adhesions
Actin cytoskeleton
Magnetic tweezers
Traction microscopy
Immunofluorescence

ABSTRACT

This study evaluates the influence of vinculin in closed conformation on the mechanical properties of cells. We demonstrate that MEFvin$^{-/-}$ cells transfected with the eGFP-vinculin mutant A50I (talin-binding-deficient-vinculin in a constitutively closed conformation) show 2-fold lower stiffness and focal adhesion density compared to MEFvin$^{+/+}$ and MEF^{Rescue} cells. MEF^{A50I} cells are as stiff as MEFvin$^{-/-}$ cells with similar focal adhesion density. Further, 2D traction microscopy indicates that MEF^{A50I} and MEFvin$^{-/-}$ cells generate 3- to 4-fold less strain energy than MEFvin$^{+/+}$ and MEF^{Rescue} cells. These results demonstrate that vinculin's mechano-coupling function is dependent on its conformational state.

1. Introduction

Adhesion is important for ensuring cell survival and proliferation. This attachment is driven by extracellular matrix contacts (EMC), which trigger biochemical/biomechanical signals inside the cell. The ~116 kDa vinculin molecule with its larger head and smaller tail domain is one of the pivotal proteins for focal adhesion formation and for its maintenance and regulation [1,2]. Vinculin is known to act as a mechano-coupler that connects the actin cytoskeleton *via* talin to the integrin-receptor [3–7]. Vinculin-deficient cells are still able to form focal contacts, however, they are more motile and less adhesive than wildtype cells [8–10]. Furthermore, vinculin-deficient cells are less stiff and generate fewer tractions in 2D and 3D than wildtype cells [11,12].

The vinculin molecule itself is a highly conserved intracellular protein which exists in two different conformations [13,14]. In the closed or autoinhibited form the vinculin head keeps the tail region picer-like in place [13–15]. In that state, binding of the vinculin tail to its binding partners is not possible. Talin or α-actinin (hydrophobic) binding to the head region (residues 1–258) activates and transfers vinculin to the open conformation [14,16,17]. This decreases the affinity between the vinculin head and tail, which allows for binding of paxillin, actin, and phospholipids [1]. FRET experiments demonstrated that vinculin must be in the open conformation for focal adhesion recruitment [16]. Mutating alanine at position 50 on vinculin to isoleucine (A50I) prevents talin binding [13,18]. This mutation inhibits head/tail dissociation of vinculin and increases the vinculin turnover rate in focal adhesions (FAs) [18]. Weakening the head/tail interaction by mutating certain residues at the contact surface between head and tail (e.g. D974, K975, R976, R978A) is shifting vinculin to a constitutively open state. Cells transfected with these vinculin mutants showed more focal adhesions in comparison to wildtype cells [18,19].

To further analyze vinculin's role as mechano-coupler, we used the A50I vinculin variant in magnetic tweezer and 2D-traction microscopic experiments. In additional experiments, we counted the number of focal adhesions for each cell type of similar size. The results suggest that force transmission is dependent on the number of focal adhesions, and that vinculin must be in an open conformation (i.e. incorporated in the focal adhesion complex) to transmit forces *via* the actin network for cell adhesion.

2. Materials and methods

2.1. Cell culture

MEF cell lines were maintained in a low glucose (1 g/L) Dulbecco's modified Eagle's complete medium (Biochrom, Berlin, Germany) supplemented with 10% fetal calf serum (low endotoxin), 2 mM L-glutamine, and 100 U/mL penicillin/streptomycin and kept at 37 °C with 5% CO_2.

2.2. Cloning and expression of vinculin

Mouse vinculin-encoding cDNA was kindly provided by Dr. E.D. Adamson. To distinguish transfected from non-transfected cells, an eGFP cassette was cloned into pcDNA3.1 eukaryotic expression

* Corresponding author. Fax: +49 0 9131 85 25601.
E-mail address: wgoldmann@biomed.uni-erlangen.de (W.H. Goldmann).

0006-291X/$ - see front matter © 2011 Elsevier Inc. All rights reserved.
doi:10.1016/j.bbrc.2011.01.115

vector (Invitrogen, Karlsruhe, Germany), using NheI and XhoI restriction sites. The polymerase-chain-reaction amplified vinculin wild-type (1–1066), and constructs were N-terminally fused to the eGFP cassette using AflII and XbaI restriction sites. The fused eGFP constructs are driven by a CMV promoter (Clontech, Mountain View, CA). The A50I variant of vinculin was generated by the exchange of alanine (A) on position 50 to isoleucine (point mutation) using site-directed mutagenesis. To transfect cells, 2×10^5 cells were seeded in a 30 mm Ø tissue culture dish for 24 h. The cells were then transfected with 4 μg DNA using Lipofectamine (Invitrogen, Karlsruhe, Germany). Before fluorescence microscopic and tweezer measurements, approximately 2×10^5 transfected cells were reseeded in a 30 mm Ø dish or on fibronectin-coated coverslips, respectively.

2.3. Magnetic tweezer experiments

We used a magnetic tweezer device as described in [20]. For measurements, 2×10^5 cells were seeded overnight into a 30 mm Ø tissue culture dish. Thirty minutes before the experiments, the cells were incubated with fibronectin-coated paramagnetic beads of 4.5 μm Ø (Invitrogen, Karlsruhe, Germany). A magnetic field was generated using a solenoid with a needle-shaped core (HyMu80 alloy, Carpenter, Reading, PA). The needle tip was placed at a distance of 20–30 μm from a bead bound to the cell using a motorized micromanipulator (Injectman NI-2, Eppendorf, Hamburg, Germany). During measurements, bright-field images were taken by a CCD camera (ORCA ER, Hamamatsu) at a rate of 40 frames/s. The bead position was tracked on-line using an intensity-weighted center-of-mass algorithm. Measurements on multiple beads per well were performed at 37 °C for 1 h, using a heated microscope stage on an inverted microscope at 40× magnification (NA 0.6) under bright-field illumination. Transfected MEFvin$^{-/-}$ cells were identified in fluorescence mode.

2.4. 2D-traction microscopy

Different MEFs were plated overnight onto collagen-coated polyacrylamide hydrogels (Young's modulus of ~13,000 Pa) at 37 °C and 5% CO_2 in DMEM medium. Gels were prepared according to a modified protocol by Pelham and Wang [21]. Adherent cells were detached by treating them with cytochalasin D and trypsin. The gel relaxed into an undeformed state after cell detachment. Comparing the position of fluorescent microspheres in the deformed and undeformed state, the traction field can be obtained using a difference-with-interpolation algorithm with a spatial resolution of 2.5 μm and an accuracy of 8 nm. Tractions were computed according to a Fourier-based-algorithm [22] and expressed as elastic strain energy of the matrix.

3. Results and discussion

The focal adhesion protein vinculin (1066 residues) with its head (residues 1–821) and tail (residues 858–1066) domains exhibits a bistable behavior, operating in either an open or a closed conformation. It is believed that (i) in the closed state, intramolecular interactions between the head and tail obstruct the exposure of cryptic binding sites for proteins and surface binding sites for phospholipids and (ii) in the open state, when the head and tail are dissociated, the cryptic binding sites in the helical bundles are exposed [13,18,19,23]. The dissociation is assumed to be cooperative, and the activation is most likely to be allosteric. According to Chen et al. [16] several conformational states are likely, exposing different combinations of cryptic binding sites for other focal adhesion proteins during the turnover of focal adhesion complexes, which changes cellular dynamic behavior.

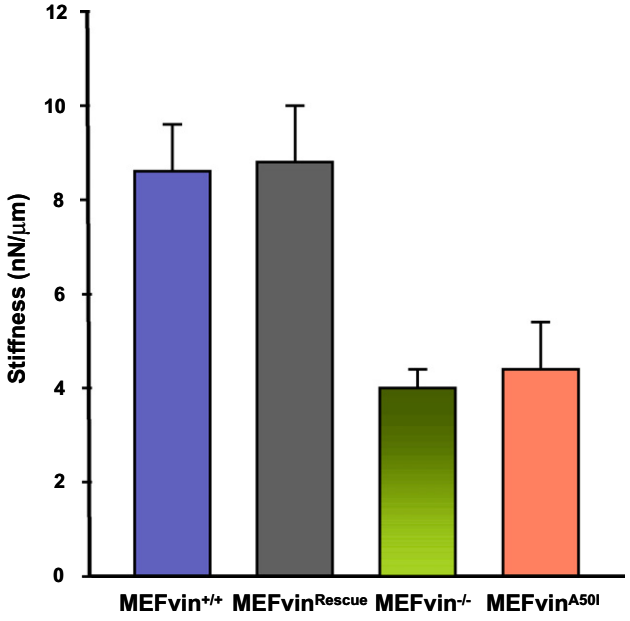

Fig. 1. Magnetic tweezer measurements of MEFvin$^{+/+}$ (blue), MEF^{Rescue} (black), MEFvin$^{-/-}$ (green), and MEFvin^{A50I} (orange) cells. All cells were incubated with fibronectin-coated superparamagnetic beads (Ø 4.5 μm) for 30 min, after which the paramagnetic beads were displaced from their original position by 2 nN force of the magnetic tweezer. Displacement $D(t)$ of the bead followed the relation, $D(t) = 2\ \mathrm{nN} \times a(t/t_0)^b$, where the parameter $1/a$ (units of nN/μm) characterizes the cell stiffness. MEFvin$^{+/+}$ and MEF^{Rescue} cells were about twofold stiffer than MEFvin$^{-/-}$ and MEFvin^{A50I} cells. The standard error of the mean (SEM) is indicated by the bars; the number of cells analyzed per cell line were between 65 and 85. (For interpretation of the references to color in this figure legend, the reader is referred to the web version of this article.)

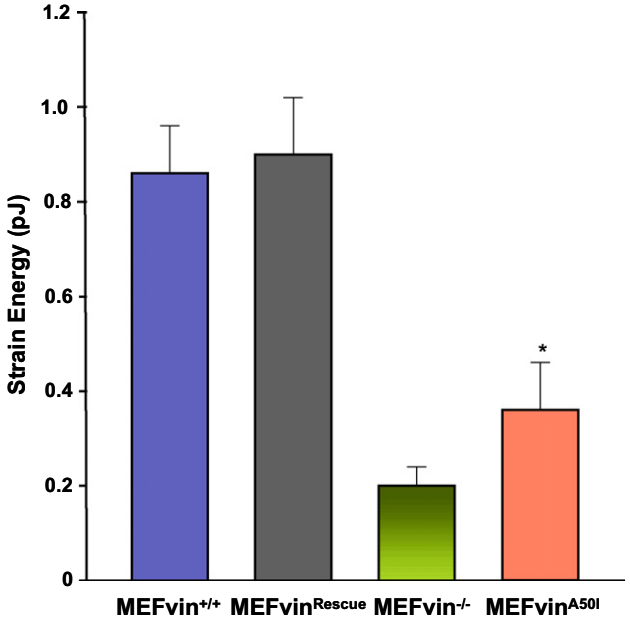

Fig. 2. 2D traction microscopy of MEFvin$^{+/+}$, MEF^{Rescue}, MEFvin$^{-/-}$, and MEFvin^{A50I} cells. All cells were seeded on collagen-coated elastic substrates (~13 kPa) and tractions were determined. The strain energy of both MEFvin$^{+/+}$ and MEF^{Rescue} cells was about 4-fold higher than MEFvin$^{-/-}$ cells and approximately 3-fold higher than MEFvin^{A50I} cells. The standard error of the mean (SEM) is indicated by the bars; the number of cells analyzed per cell line were between 30 and 80; $^*p < 0.05$.

In this study, we mutated alanine on position 50 of the vinculin molecule to an isoleucine (A50I) to prevent the protein talin from binding and to maintain the vinculin molecule in a closed state [13,18]. To test cell mechanical changes induced by an open *vs.* closed conformation, we measured the cell stiffness of MEF vinculin variants using the magnetic tweezer device (Fig. 1). We observed that the tentatively open wildtype/rescue (MEFvin$^{+/+}$/MEF^{Rescue}) cells *vs.* the closed MEFvin^{A50I} cells were about twofold stiffer at 2 nN force. The stiffness of vinculin-deficient (MEFvin$^{-/-}$) cells was similar to that of MEFvin^{A50I} mutant cells. These results support the hypothesis that in the closed state (A50I) of vinculin, the binding of other focal adhesion proteins is compromised, and that the binding sites for other focal adhesion proteins on vinculin are only accessible in the open state of vinculin [18]. Two-dimensional traction microscopic measurements further support this view. We could demonstrate that the contractile forces generated *via* the intracellular integrin-FA-actomyosin link are 3–4-fold higher in MEFvin$^{+/+}$ and MEF^{Rescue} cells compared to MEFvin^{A50I} and MEFvin$^{-/-}$ cells (Fig. 2). Previously, it was reported that focal adhesion formation depends on internal tension [2,11,24,25]. We determined the number of focal adhesions in MEF cell lines of similar spreading area (Fig. 3). MEFvin$^{+/+}$ and MEF^{Rescue} cells showed similar density of focal adhesions, whereas MEFvin^{A50I} and MEFvin$^{-/-}$ cells showed between 40%–50% fewer focal adhesions. The size of the focal adhesions in these different cell lines was similar (Fig. 4). These results support the view that the reduced focal adhesion density in MEFvin^{A50I} and MEFvin$^{-/-}$ compared to MEFvin$^{+/+}$ and MEF^{Rescue} cells might be a secondary effect due to the reduced force generation [11].

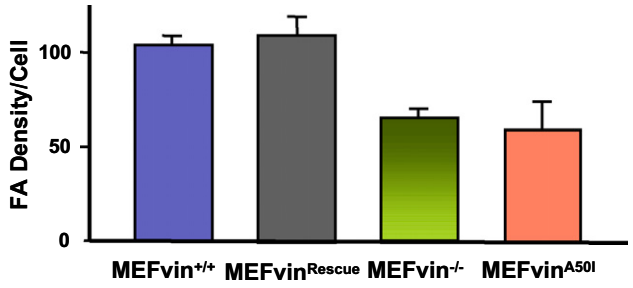

Fig. 3. Focal adhesion (FA) density per cell line determined from confocal microscopic images. Only cells of similar spreading area were analyzed, showing about 110 FAs for MEFvin$^{+/+}$ and 115 for MEF^{Rescue} cells, about 65 FAs for MEFvin$^{-/-}$, and around 58 FAs for MEFvin^{A50I} cells. The number of cells analyzed was between 23 and 49. The standard error of the mean (SEM) is indicated by the bars.

The interaction of vinculin with other focal adhesion proteins like α-actinin, α- and/or β-catenin, and/or talin as well as vinculin phosphorylation have been reported to influence vinculin's linkage with the actin cytoskeleton to allow for cellular force generation [7,11,26–29]. It has previously been reported that the A50I mutation in vinculin head ablated talin binding due to steric hindrance and that the loss of talin binding correlated with significant enhancement of vinculin dynamics in focal adhesions [18,30]. These reports concluded that the high vinculin dynamics is characteristic of the head domain that requires the talin binding site for vinculin activation and proper FA incorporation. All these findings point into the direction of a distinct state (open or closed) of vinculin which has mechanical implications on the cell behavior. In summary, only the open

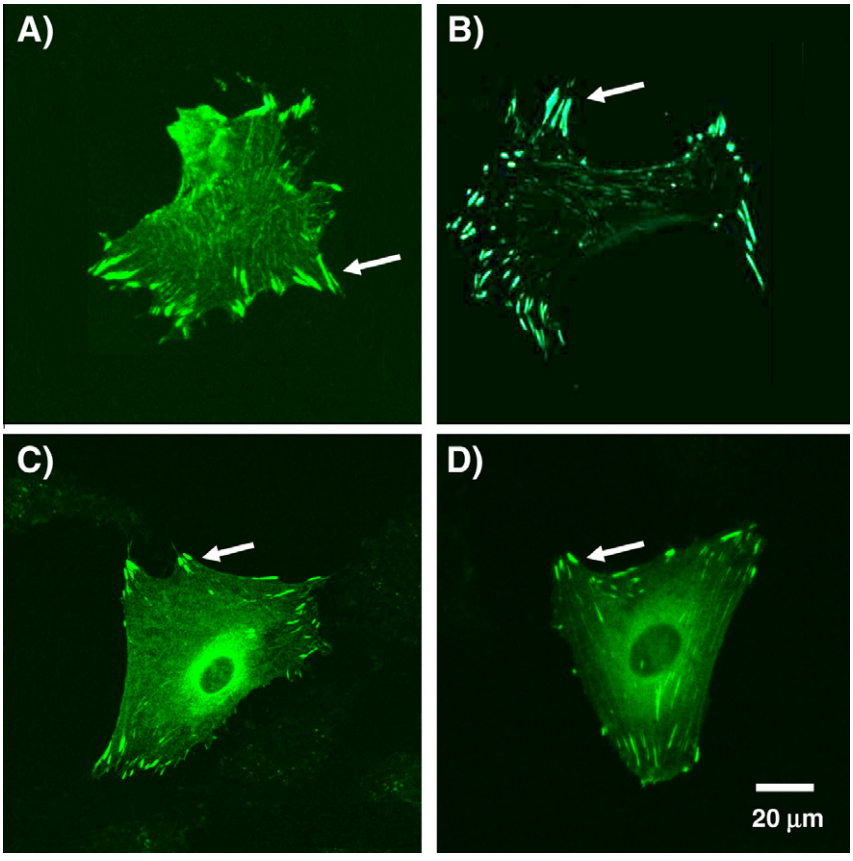

Fig. 4. Confocal microscopic images of 20× magnification show focal adhesions (arrows) in MEFs. MEFvin$^{+/+}$ as well as transfected and non-transfected MEFvin$^{-/-}$ cells were seeded on fibronectin-coated glass slides and allowed to adhere overnight. The focal adhesions in MEFvin$^{+/+}$ (A) and MEFvin$^{-/-}$ (C) cells were stained with antibodies against paxillin; in MEF^{Rescue} (B) and MEFvin^{A50I} (D) cells, focal adhesions were determined using a N-terminal eGFP label.

conformation of vinculin facilitates contractile force generation and proper focal adhesion formation in cells.

Further detailed experimental studies are still needed to answer the following questions: (i) what is the influence of vinculin's phosphorylation on the binding of talin and actin to vinculin and (ii) how does vinculin's activation influence the mechanical load (i.e. strengthening and reinforcement) of focal adhesions.

Acknowledgments

We thank Drs. Bernd Hoffmann, Anna Klemm, and Jose Luis Alonso for stimulating discussions. This work was supported by grants from Bayerisch–Französisches Hochschulzentrum, Deutscher Akademischer Austausch Dienst, Bavaria California Technology Center, and Deutsche Forschungsgemeinschaft.

References

[1] W.H. Ziegler, R.C. Liddington, D.R. Critchley, The structure and regulation of vinculin, Trends Cell Biol. 16 (2006) 453–460.
[2] C. Möhl, N. Kirchgessner, C. Schafer, K. Kupper, S. Born, G. Diez, W.H. Goldmann, R. Merkel, B. Hoffmann, Becoming stable and strong: the interplay between vinculin exchange dynamics and adhesion strength during adhesion site maturation, Cell Motil. Cytoskel. 66 (2009) 350–364.
[3] W.H. Goldmann, M. Schindl, T.J. Cardozo, R.M. Ezzell, Motility of vinculin-deficient F9 embryonic carcinoma cells analyzed by video, laser confocal, and reflection interference contrast microscopy, Exp. Cell Res. 221 (1995) 311–319.
[4] W.H. Goldmann, R.M. Ezzell, Viscoelasticity in wild-type and vinculin-deficient (5.51) mouse F9 embryonic carcinoma cells examined by atomic force microscopy and rheology, Exp. Cell Res. 226 (1996) 234–237.
[5] R.M. Ezzell, W.H. Goldmann, N. Wang, N. Parasharama, D.E. Ingber, Vinculin promotes cell spreading by mechanically coupling integrins to the cytoskeleton, Exp. Cell Res. 231 (1997) 14–26.
[6] W.H. Goldmann, R. Galneder, M. Ludwig, W. Xu, E.D. Adamson, N. Wang, R.M. Ezzell, Differences in elasticity of vinculin-deficient F9 cells measured by magnetometry and atomic force microscopy, Exp. Cell Res. 239 (1998) 235–242.
[7] C.T. Mierke, P. Kollmannsberger, D. Paranhos-Zitterbart, J. Smith, B. Fabry, W.H. Goldmann, Mechano-coupling and regulation of contractility by the vinculin tail domain, Biophys. J. 94 (2008) 661–670.
[8] J.L. Coll, A. Ben-Ze'ev, R.M. Ezzell, J.L. Rodriguez Fernandez, H. Baribault, R.G. Oshima, E.D. Adamson, Targeted disruption of vinculin genes in F9 and embryonic stem cells changes cell morphology, adhesion, and locomotion, Proc. Natl. Acad. Sci. USA 92 (1995) 9161–9165.
[9] W. Xu, H. Baribault, E.D. Adamson, Vinculin knockout results in heart and brain defects during embryonic development, Development 125 (1998) 327–337.
[10] W. Xu, J.L. Coll, E.D. Adamson, Rescue of the mutant phenotype by reexpression of full-length vinculin in null F9 cells; effects on cell locomotion by domain deleted vinculin, J. Cell Sci. 111 (1998) 1535–1544.
[11] G. Diez, P. Kollmannsberger, C.T. Mierke, T.M. Koch, H. Vali, B. Fabry, W.H. Goldmann, Anchorage of vinculin to lipid membranes influences cell mechanical properties, Biophys. J. 97 (2009) 3105–3112.
[12] C.T. Mierke, P. Kollmannsberger, D.P. Zitterbart, G. Diez, T.M. Koch, S. Marg, W.H. Ziegler, W.H. Goldmann, B. Fabry, Vinculin facilitates cell invasion into three-dimensional collagen matrices, J. Biol. Chem. 285 (2010) 13121–13130.
[13] C. Bakolitsa, D.M. Cohen, L.A. Bankston, A.A. Bobkov, G.W. Cadwell, L. Jennings, D.R. Critchley, S.W. Craig, R.C. Liddington, Structural basis for vinculin activation at sites of cell adhesion, Nature 430 (2004) 583–586.
[14] T. Izard, G. Evans, R.A. Borgon, C.L. Rush, G. Bricogne, P.R. Bois, Vinculin activation by talin through helical bundle conversion, Nature 427 (2004) 171–175.
[15] W.H. Ziegler, A.R. Gingras, D.R. Critchley, J. Emsley, Integrin connections to the cytoskeleton through talin and vinculin, Biochem. Soc. Trans. 36 (2008) 235–239.
[16] H. Chen, D.M. Cohen, D.M. Choudhury, N. Kioka, S.W. Craig, Spatial distribution and functional significance of activated vinculin in living cells, J. Cell Biol. 169 (2005) 459–470.
[17] P.R. Bois, B.P. O'Hara, D. Nietlispach, J. Kirkpatrick, T. Izard, The vinculin binding sites of talin and alpha-actinin are sufficient to activate vinculin, J. Biol. Chem. 281 (2006) 7228–7236.
[18] D.M. Cohen, B. Kutscher, H. Chen, D.B. Murphy, S.W. Craig, A conformational switch in vinculin drives formation and dynamics of a talin-vinculin complex at focal adhesions, J. Biol. Chem. 281 (2006) 16006–16015.
[19] D.M. Cohen, R.P. Johnson, B. Choudhury, S.W. Craig, Two distinct head–tail interfaces cooperate to suppress activation of vinculin by talin, J. Biol. Chem. 280 (2005) 17109–17117.
[20] P. Kollmannsberger, B. Fabry, High-force magnetic tweezers with force feedback for biological applications, Rev. Sci. Instrum. 78 (2007) 114301–114306.
[21] R.J. Pelham Jr., Y.L. Wang, Cell locomotion and focal adhesions are regulated by the mechanical properties of the substrate, Biol. Bull. 194 (1998) 348–349. discussion 349–350.
[22] J.P. Butler, I.M. Tolic-Norrelykke, B. Fabry, J.J. Fredberg, Traction fields, moments, and strain energy that cells exert on their surroundings, Am. J. Physiol. Cell Physiol. 282 (2002) C595–605.
[23] M. Himmel, A. Ritter, S. Rothemund, B.V. Pauling, K. Rottner, A.R. Gingras, W.H. Ziegler, Control of high affinity interactions in the talin C terminus: how talin domains coordinate protein dynamics in cell adhesions, J. Biol. Chem. 284 (2009) 13832–13842.
[24] N.Q. Balaban, U.S. Schwarz, D. Riveline, P. Goichberg, G. Tzur, I. Sabanay, D. Mahalu, S. Safran, A. Bershadsky, L. Addadi, B. Geiger, Force and focal adhesion assembly: a close relationship studied using elastic micropatterned substrates, Nat. Cell Biol. 3 (2001) 466–472.
[25] A.D. Bershadsky, N.Q. Balaban, B. Geiger, Adhesion-dependent cell mechano sensitivity, Annu. Rev. Cell Dev. Biol. 19 (2003) 677–695.
[26] R.P. Johnson, S.W. Craig, An intramolecular association between the head and tail domains of vinculin modulates talin binding, J. Biol. Chem. 269 (1994) 12611–12619.
[27] R.P. Johnson, S.W. Craig, F-actin binding site masked by the intramolecular association of vinculin head and tail domains, Nature 373 (1995) 261–264.
[28] Z. Zhang, G. Izaguirre, S.Y. Lin, H.Y. Lee, E. Schaefer, B. Haimovich, The phosphorylation of vinculin on tyrosine residues 100 and 1065, mediated by SRC kinases, affects cell spreading, Mol. Biol. Cell 15 (2004) 4234–4247.
[29] X. Peng, L.E. Cuff, C.D. Lawton, K.A. DeMali, Vinculin regulates cell-surface E-cadherin expression by binding to beta-catenin, J. Cell Sci. 123 (2009) 567–577.
[30] J. Golji, J. Lam, M.R. Mofrad, Vinculin activation is necessary for complete talin binding, Biophys. J. 100 (2011) 332–340.